

Complete and incomplete fusion of weakly bound nuclei

H. D. Marta,^{1,*} L. F. Canto,² and R. Donangelo^{1,2}

¹*Instituto de Física, Facultad de Ingeniería, C.C. 30, 11000 Montevideo, Uruguay*

²*Instituto de Física, Universidade Federal do Rio de Janeiro, Rio de Janeiro, Rio de Janeiro, Brazil*

(Received 31 August 2013; revised manuscript received 24 February 2014; published 27 March 2014)

Existing quantum mechanics methods to study fusion reactions with weakly bound nuclei cannot evaluate separately the complete fusion and the incomplete fusion cross sections. We develop a semiclassical procedure that can calculate these cross sections, apply it to ${}^6\text{Li} + {}^{209}\text{Bi}$ collisions at energies just above the barrier, and show that its predictions for the different fusion cross sections are in good agreement with the data. We find that the contribution from the sequential fusion of the Li fragments to the complete fusion cross section is substantial in the case of ${}^6\text{Li}$, reaching almost 40% of that from the direct process, which illustrates the importance of calculating correctly the different components of the fusion cross section.

DOI: [10.1103/PhysRevC.89.034625](https://doi.org/10.1103/PhysRevC.89.034625)

PACS number(s): 25.70.Jj, 24.10.Eq, 25.70.Mn

I. INTRODUCTION

The availability of radioactive beams opened new possibilities in nuclear physics. In particular, collisions of weakly bound nuclei have aroused great interest, both theoretical and experimental, over the past decade [1]. In such collisions, the breakup cross section tends to be very large and breakup couplings may have a strong influence on the cross sections for several other channels. An important example is the fusion process, which in this case becomes much more complex, as, in addition to the usual fusion reaction, in which the whole projectile merges with the target to form the compound nucleus, there are other fusion processes following the breakup of the weakly bound collision partner. There is the possibility that one or more, but not all, fragments are absorbed by the target, whereas part of the projectile's mass escapes the interaction region. It can also happen that all the projectile's fragments are sequentially absorbed by the target, producing the same compound nucleus as in the case of direct fusion. These fusion processes receive different names. When the compound nucleus does not contain all of the projectile's nucleons, we employ the term *incomplete fusion* (ICF), whereas the fusion of all of the projectile's nucleons with the target is called *complete fusion* (CF). The CF cross section is the sum of the cross section for the direct fusion of the projectile with the target (DCF) and of the sequential fusion of all of the projectile's fragments (SCF).

Most experiments measure only the total fusion (TF) cross section, which is the sum of the cross sections for CF and ICF. However, for some particular projectile-target combinations, it is possible to perform separate measurements of the cross sections for CF and ICF. Important examples are the fusion reactions ${}^6,7\text{Li} + {}^{209}\text{Bi}$ [2,3] and ${}^9\text{Be} + {}^{208}\text{Pb}$ [3,4], where the influence of the breakup channel on fusion was shown to be very strong.

Many theoretical approaches have been proposed to study fusion reactions with weakly bound nuclei (for a review see Ref. [1]), ranging from simple classical models [5,6]

to full quantum-mechanical calculations [7–10], using the continuum discretized coupled channel method (CDCC). In most CDCC calculations fusion is included by means of short-range imaginary potentials acting on each fragment. In this way, there is no correlation between absorptions of different fragments. Thus, one cannot know if the absorption by one of these potentials contributes to ICF or to CF. Consequently, the calculation gives only the summed cross section for these processes, σ_{TF} [11]. This shortcoming is avoided in the CDCC calculations of Hagino *et al.* [7] and Diaz-Torres and Thompson [8]. These works adopt a single imaginary potential acting on the full projectile and attribute absorption in the bound channels to CF and absorption in channels in the continuum to ICF. However, this procedure may only be in some way justified when the absorbed fragment contains a large fraction of the projectile's mass. In this case, the center of mass of the projectile is very close to the center of mass of the heavy fragment, and it may be a good approximation to assume that the heavy fragment is absorbed whenever the projectile is inside the range of the imaginary potential. This is the case of ${}^{11}\text{Be}$, which was the projectile in the calculations of Refs. [7,8]. In this case, the breakup reaction is ${}^{11}\text{Be} \rightarrow n + {}^{10}\text{Be}$ and ICF corresponds to the fusion of the ${}^{10}\text{Be}$ fragment with the target. However, this procedure cannot be used when the projectile dissociates into fragments of comparable masses. In such cases, a projectile-target imaginary potential for unbound channels is meaningless. The center of mass of the projectile of the dissociated projectile may be inside the range of the imaginary potential with the two fragments being far away. Therefore, there are no quantum-mechanical methods to evaluate CF and ICF cross sections for collisions of weakly bound projectiles that break up into fragments of comparable masses, like ${}^6,7\text{Li}$ or ${}^9\text{Be}$, and the development of new methods to evaluate CF and ICF cross sections that incorporate quantum effects is called for.

In the present work, we introduce a semiclassical method to evaluate CF and ICF cross sections in collisions of weakly bound nuclei. Our method, which has been successfully applied to breakup reactions [12], consists of treating the projectile-target relative motion by classical mechanics while the intrinsic dynamics of the weakly bound projectile is

*Deceased

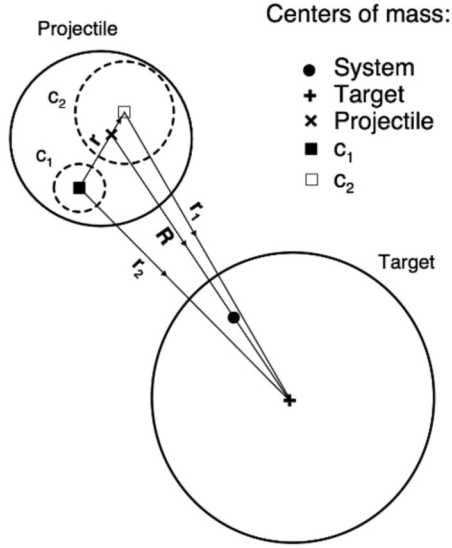


FIG. 1. Coordinates used in the main text to describe the breakup reaction of a weakly bound projectile by a heavy target.

handled by quantum mechanics. In Sec. II we give the details of the method, in particular the separate calculation of the complete and ICF cross sections. The results of this procedure applied to the collisions of ${}^6,7\text{Li}$ ions incident on ${}^{209}\text{Bi}$ are presented in Sec. III. Conclusions and possible extensions of this work are drawn in the last section of this work.

II. CALCULATION PROCEDURE

We consider the reaction as a two-step process. In the first part the breakup of the weakly bound projectile is described by the semiclassical procedure of Refs. [12,13]. The breakup amplitudes obtained are transformed to momentum distributions of the fragments, and we use this information to calculate the fusion probabilities of the breakup products. In the following we consider in more detail these aspects of the semiclassical calculation.

A. Amplitudes

We begin by summarizing the breakup part of the process. As in our previous works [12,13], we consider a weakly bound projectile consisting of two clusters, c_1 and c_2 , moving around the projectile's center of mass. The collision dynamics is described by two vectors: \mathbf{R} , joining the centers of mass of the projectile and the target, and \mathbf{r} , joining the centers of c_1 and c_2 . This is illustrated in Fig. 1. As the collision proceeds, the projectile-target interaction couples the intrinsic states of the system. In this way, the projectile, which is initially in its ground state, may suffer transitions to excited bound states, if any, and to continuum states. For a collision with given energy, E , and impact parameter, b , one determines a trajectory by classical mechanics and uses this trajectory to transform \mathbf{R} dependence into time dependence. The intrinsic dynamics is then treated as a time-dependent quantum-mechanics problem.

Analogously to Refs. [14,15], the interaction is given in terms of the fragment-target vectors,

$$\mathbf{r}_1 = \mathbf{R} + \frac{A_2}{A_P} \mathbf{r}, \quad \mathbf{r}_2 = \mathbf{R} - \frac{A_1}{A_P} \mathbf{r},$$

by the expression

$$V(\mathbf{R}, \mathbf{r}) = V_1 \left(\mathbf{R} + \frac{A_2}{A_P} \mathbf{r} \right) + V_2 \left(\mathbf{R} - \frac{A_1}{A_P} \mathbf{r} \right), \quad (1)$$

where V_1 (V_2) is the interaction between c_1 (c_2) and the target. Above, A_1 and A_2 are the mass numbers of c_1 and c_2 , and $A_P = A_1 + A_2$ is the mass number of the projectile. The potentials V_1 and V_2 contain nuclear and Coulomb parts. For the semiclassical calculation, as in Ref. [12], the interaction is split into an optical potential, V_0 , the real part of which only affects the classical trajectory of the projectile-target system, while its imaginary part represents absorption from other channels, and a coupling interaction, $U(\mathbf{R}, \mathbf{r})$, which leads to breakup,

$$V_0(\mathbf{R}) = V(\mathbf{R}, \mathbf{r} = 0) = V_1(\mathbf{R}) + V_2(\mathbf{R}) \quad (2)$$

and

$$U(\mathbf{R}, \mathbf{r}) = V(\mathbf{R}, \mathbf{r}) - \text{Re} \{ V_0(\mathbf{R}) \}. \quad (3)$$

The derivation of the semiclassical coupled-channel equations was done in Sec. II of Ref. [12], where also the procedure for the discretization of the continuum was described in detail. In summary, the time-dependent wave function describing the c_1 - c_2 relative motion in the projectile frame is expanded as

$$\Psi(b, t) = \sum_i c_i(b, t) \psi_i e^{-i\varepsilon_i t/\hbar} + \Psi_c(b, t), \quad (4)$$

where $c_i(b, t)$ are the amplitudes associated with the bound states, ψ_i , and $\Psi_c(b, t)$ is the component of $\Psi(b, t)$ in the continuum,

$$\Psi_c(b, t) = \sum_{l_\alpha j_\alpha J_\alpha M_\alpha} \int d\varepsilon_\alpha c_\alpha(b, t) e^{-i\varepsilon_\alpha t/\hbar} \Psi_\alpha. \quad (5)$$

The amplitudes $c_\alpha(b, t)$ are associated with the basis states in the continuum discretization, Ψ_α .

The study of the breakup follows the same procedure as in that work. In the present paper we study the evolution of the system after the breakup took place, in particular the eventual fusion of one or both of the projectile fragments with the target nucleus.

To do this, as we have the breakup amplitudes $c_\alpha(b, t)$ along the projectile trajectory, we could, in principle, consider, at each point along that trajectory, that the two clusters appear with the velocities associated with the continuum state α and probabilities $|c_\alpha(b, t)|^2$. These are the initial conditions needed to determine whether those clusters fuse with the target nucleus.

Although the above procedure is feasible, it would require the evaluation of a very large number of fusion probabilities. To decrease the computational effort of the calculation, we have resorted to the following approximation. We calculate the breakup amplitudes of Eq. (5) until the classical trajectory reaches the point of closest approach. We then consider that,

when breakup takes place, the fragments are created at the point of closest approach of the projectile's classical trajectory. This assumption is reasonable because the breakup probability distribution is strongly peaked in the region around the point of closest approach.

B. Direct complete fusion

The DCF cross section is calculated as

$$\sigma_{\text{DCF}} = \frac{\pi}{K^2} \sum_L (2L+1) (1 - P_L^{\text{bup}}) T_L^{(\text{p})}(K), \quad (6)$$

where the factor P_L^{bup} is the breakup probability and $T_L^{(\text{p})}(K)$ is the probability that the projectile fuses with the target when having momentum $\hbar K$ in the partial wave L . The fusion probabilities are approximated by the Hill-Wheeler formula,

$$T_L^{(\text{p})}(K) = \frac{1}{1 + \exp \left\{ \frac{2\pi}{\hbar\omega_0} \left[V_{B_0} + \frac{\hbar^2}{2\mu_{\text{PT}}} \frac{(L+\frac{1}{2})^2}{r_{b_0}^2} - E \right] \right\}}. \quad (7)$$

Here, $E = \hbar^2 K^2 / 2\mu_{\text{PT}}$, where μ_{PT} is the reduced mass of the projectile-target system, and V_{B_0} , r_{b_0} , and $\hbar\omega_0$ are the height, radius, and curvature, respectively, of the barrier corresponding to the projectile-target system. When $R < r_{b_0}$ we consider $T_L^{(\text{p})}(K) = 1$.

C. Incomplete fusion and sequential complete fusion

We calculate the ICF cross section of fragment c_i , $i = 1, 2$ by means of the expression

$$\sigma_{\text{ICF}_i} = \frac{\pi}{K^2} \sum_L (2L+1) \int d^3\mathbf{k} |A^L(\mathbf{k})|^2 P_{F_i}(\mathbf{k}), \quad (8)$$

and the SCF cross section is

$$\sigma_{\text{SCF}} = \frac{\pi}{K^2} \sum_L (2L+1) \int d^3\mathbf{k} |A^L(\mathbf{k})|^2 P_{\text{SCF}}(\mathbf{k}). \quad (9)$$

Above,

$$A^L(\mathbf{k}) = \sum_{v_1 v_2} A_{v_1 v_2}(\mathbf{k}, t_f, b) \quad (10)$$

is the relative momentum distribution of the c_1 - c_2 system at the instant of closest approach or when it enters the strong interaction region, t_f , and we denote by $\hbar K$ and $L = Kb$ the relative momentum and the orbital angular momentum in units of \hbar of the projectile-target relative motion, respectively. In Eq. (10), $A_{v_1 v_2}(\mathbf{k}, t, b)$ is the scalar product

$$A_{v_1 v_2}(\mathbf{k}, t, b) = \langle \Psi_{v_1 v_2}^{(-)}(\mathbf{k}, t) | \Psi_c(b, t) \rangle,$$

where the wave function $\Psi_c(b, t)$ is given by Eq. (5) and $\Psi_{v_1 v_2}^{(-)}(\mathbf{k}, t)$ is the scattering wave function with incoming wave boundary conditions. It is given by

$$\Psi_{v_1 v_2}^{(-)}(\mathbf{k}, t) = \mathcal{T} \Psi_{-v_1 -v_2}^{(+)}(-\mathbf{k}, -t), \quad (11)$$

where \mathcal{T} is the time-reversal operator and $\Psi_{v_1 v_2}^{(+)}(\mathbf{k}, t) = \Psi_{v_1 v_2}^{(+)}(\mathbf{k}) \exp(-i\varepsilon_k t / \hbar)$ is the scattering wave function with outgoing wave boundary conditions, with $\varepsilon = \hbar^2 k^2 / 2\mu_{12}$,

In Eq. (8), $P_{F_i}(\mathbf{k})$ is the probability that only the fragment c_i ($i = 1, 2$) fuses with the target, given by

$$P_{F_1}(\mathbf{k}) = T_{l_1}^{(c_1)}(E_1) [1 - T_{l_2}^{(c_2)}(E_2)], \quad (12)$$

$$P_{F_2}(\mathbf{k}) = T_{l_2}^{(c_2)}(E_2) [1 - T_{l_1}^{(c_1)}(E_1)], \quad (13)$$

In Eq. (9), $P_{\text{SCF}}(\mathbf{k})$ is the probability that both fragments fuse with the target,

$$P_{\text{SCF}}(\mathbf{k}) = T_{l_1}^{(c_1)}(E_1) T_{l_2}^{(c_2)}(E_2). \quad (14)$$

In the above equations, $T_{l_i}^{(c_i)}(E_i)$ is the probability that a fragment c_i with energy E_i and angular momentum l_i tunnels through the barrier associated with its interaction with the target. Note that, in each case, $[1 - T_{l_j}^{(c_j)}(E_j)]$ is the nontunneling probability for the other fragment.

Energy conservation requires that the relative projectile-target velocity V be modified by the breakup process, $V \rightarrow V'$,

$$V' = \sqrt{V^2 - \frac{\mu_{12}}{\mu_{\text{PT}}} v^2 - \frac{2B}{\mu_{\text{PT}}}}, \quad (15)$$

where v is the modulus of the relative velocity between fragments c_1 and c_2 , μ_{12} is the reduced mass of these fragments, and where B is the breakup threshold. Besides, we make the simplifying assumption that the orientation of this velocity is conserved in such a process. The fragment velocities relative to the target are

$$\mathbf{v}_1 = \mathbf{V}' - \frac{m_2}{m_p} \mathbf{v}, \quad \mathbf{v}_2 = \mathbf{V}' + \frac{m_1}{m_p} \mathbf{v}, \quad (16)$$

the energy of the c_i -target relative motion is given by

$$E_i = \frac{1}{2} \mu_i v_i^2 + V_i(\mathbf{r}_i), \quad (17)$$

where μ_i is the reduced mass of the fragment c_i -target system and $V_i(\mathbf{r}_i)$ is the interaction between these two nuclei at the position of the fragment c_i when the fusion calculation begins. The angular momentum of the c_i -target system with respect to its center of mass is

$$\hbar \mathbf{l}_i = \mu_i \mathbf{r}_i \times \mathbf{v}_i. \quad (18)$$

For the fragment c_1 this results in

$$\mathbf{l}_1 = \frac{\mu_1}{\hbar} \left(\mathbf{R} - \frac{m_2}{m_p} \mathbf{r} \right) \times \mathbf{v}_1, \quad (19)$$

and analogously for fragment c_2 .

As before, the fusion probabilities are estimated by means of the Hill-Wheeler formula,

$$T_{l_i}^{(c_i)}(E_i) = \frac{1}{1 + \exp \left\{ \frac{2\pi}{\hbar\omega_i} \left[V_{B_i} + \frac{\hbar^2}{2\mu_i} \frac{(\ell_i + \frac{1}{2})^2}{r_{b_i}^2} - E_i \right] \right\}}. \quad (20)$$

Here $\ell_i = |\mathbf{l}_i|$, and V_{B_i} , r_{b_i} , and $\hbar\omega_i$ are the height, radius, and curvature, respectively, of the barrier corresponding to the c_i -target system. When $R < r_{b_i}$ we consider $T_{l_i}^{(c_i)}(E_i) = 1$.

III. RESULTS

Using the above procedure we have calculated the complete and ICF cross sections for the ${}^6,7\text{Li} + {}^{209}\text{Bi}$ systems, for which

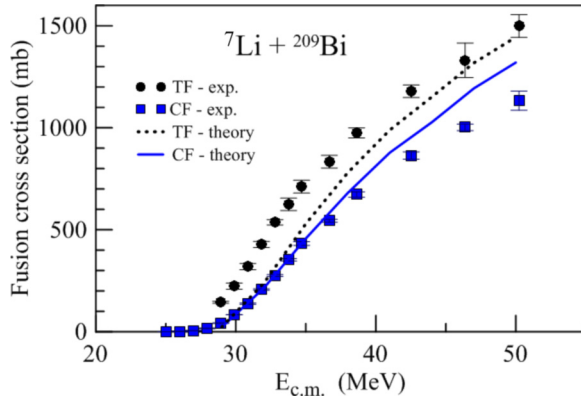


FIG. 2. (Color online) Complete and total fusion cross sections for ${}^7\text{Li}$ projectiles incident on ${}^{209}\text{Bi}$.

these data are available. For the interaction between each fragment and the target we used the Christensen-Winther potential [16,17] and the continuum discretization was performed with states with energies up to 7 MeV and angular momenta up to $3\hbar$. As our main objective is to assess the effect of the breakup channel on the CF cross section, we have not considered the different transfer processes that are found to accompany these reactions, which, as we show below, affect specially the ICF cross sections.

We start with the case of the ${}^7\text{Li}$ projectiles, which are more bound ($B = 2.47$ MeV, compared with $B = 1.47$ MeV in the case of ${}^6\text{Li}$). The potentials employed to reproduce the ground-state energies of these Li nuclides as well as the 0.48-MeV bound excited state of ${}^7\text{Li}$ were taken from Ref. [9]. In Fig. 2 we show the result of our calculations for the complete and total (complete + incomplete) fusion cross sections for the ${}^7\text{Li} + {}^{209}\text{Bi}$ system. The results shown were obtained under the assumption that, when the fusion calculation begins, the breakup fragments are no longer interacting between themselves, only with the target. We place them at the point of closest approach of the projectile c.m. trajectory, and at a distance $1.2(A_1^{1/3} + A_2^{1/3})$ fm. The orientation of the vectors joining their centers, \mathbf{r} , is given by their relative velocity. From these assumptions the initial conditions for the calculation of their fusion cross section with the target are obtained. We should remark that the fusion calculation is not very sensitive to these initial conditions: We have verified that if we start them assuming that the two fragments are emitted from the center of mass of the projectile the results do not change much. These calculations are compared with the experimental measurements of Ref. [3] of the production of residual nuclei with atomic numbers higher than that of the ${}^{209}\text{Bi}$ target in reactions induced by ${}^7\text{Li}$ projectiles.

The agreement with the CF cross section data is quite good, especially at the lower energies. However, that with the TF cross section is much poorer. The differences between the theoretical TF and CF cross sections are much smaller than those observed in the data. We believe that this is because the TF experimental cross sections do not include only CF and ICF, but also direct transfers of ${}^3\text{H}$ and ${}^4\text{He}$ clusters, which lead to the same residual nuclei as the ICF of

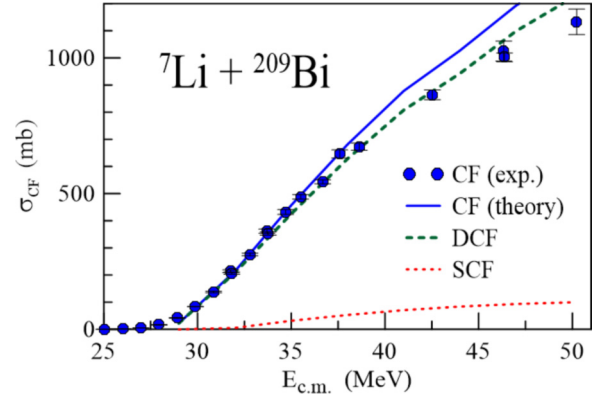


FIG. 3. (Color online) Components of the CF cross section in the case of ${}^7\text{Li}$ projectiles.

the corresponding fragment produced by ${}^7\text{Li}$ breakup. These processes and their contribution cannot be disentangled from that of the ICF in the measurements. However, from the theoretical point of view, ICF and cluster transfer are completely different processes. The former is a two-step transition (breakup followed by ICF), whereas the latter is reached in a single step.

There is also an additional complication for the theoretical description of this data. Recent experiments [18,19] on ${}^7\text{Li}$ breakup in collisions with different targets have detected a significant number of events where ${}^4\text{He}$ is in coincidence with ${}^2\text{H}$, instead of ${}^3\text{H}$. Furthermore, proton pickup, followed by the resulting ${}^8\text{Be}$ nucleus decay into two α particles, appears to be the dominant transfer mechanism leading to breakup, at least at sub-barrier energies. Thus, one-nucleon transfer channels are likely to play an important role in the reaction mechanism. The treatment reported in the present work describes only the breakup channel, and not any of the transfer channels that influence the production of the residual nuclei observed in the experiment of Ref. [3].

The CF cross section is, however, much more clearly defined from an experimental viewpoint, so we concentrate on the analysis of its components. A recent experiment of Luong *et al.* [20] has been able to distinguish prompt breakup from delayed breakup. However, there is no experiment that

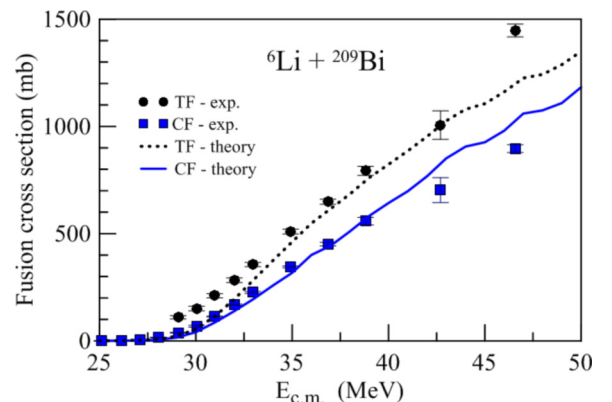
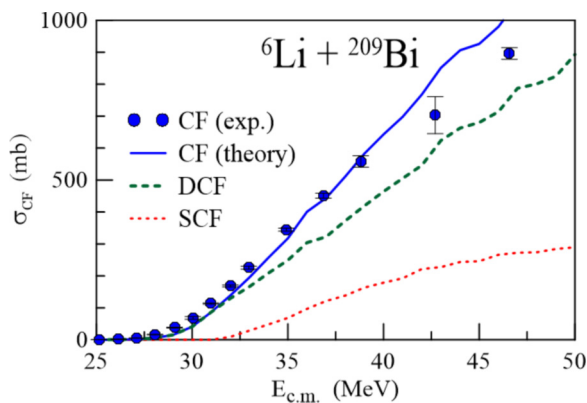
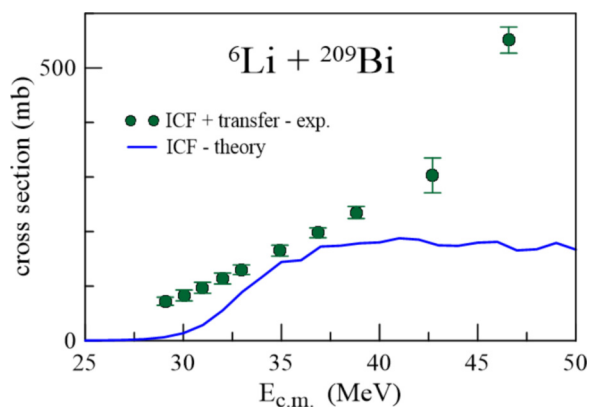


FIG. 4. (Color online) Similar to Fig. 2 for ${}^6\text{Li}$ projectiles.

FIG. 5. (Color online) Similar to Fig. 3 for ${}^6\text{Li}$ projectiles.

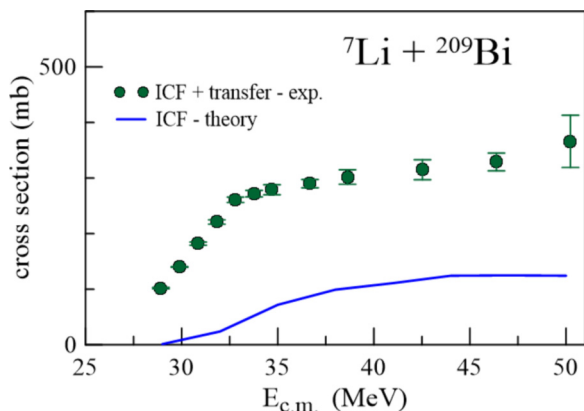
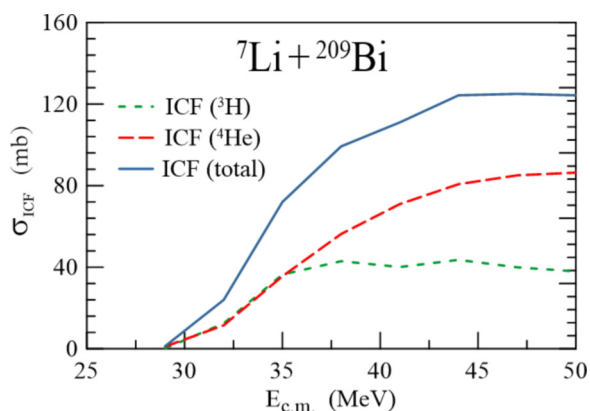
can distinguish DCF from SCF. From what we mentioned in the Introduction, if the SCF cross section were negligible, the CF cross section could be obtained from standard CDCC calculations. Because in the semiclassical approach presented here DCF and SCF can be separately calculated, we can check the importance of the latter. In Fig. 3 we show the calculated DCF and SCF cross sections, together with that of the CF (DCF + SCF). We note that, in this case, the SCF contribution is quite small. This is consistent with the expectation that breakup is not a dominant process for ${}^7\text{Li}$ projectiles, as their binding energy is not too small. In cases like this, standard CDCC calculations should correctly describe the CF cross section.

Let us now consider the case of the more weakly bound ${}^6\text{Li}$ projectiles, for which we have performed similar calculations. In Fig. 4 we show the complete and total fusion cross sections for the ${}^6\text{Li} + {}^{209}\text{Bi}$ system. The agreement with the CF cross section data is rather good, and that with the TF cross section is reasonable, except for the large differences at high energies. We give a similar interpretation to those differences as in the ${}^7\text{Li} + {}^{209}\text{Bi}$ collision. However, in the present case the calculated TF and CF cross sections differ markedly, indicating the importance of breakup channels in the fusion processes for this system. When we analyze the components of the CF

FIG. 7. (Color online) Similar to Fig. 6 for ${}^6\text{Li}$ projectiles.

cross section in the case of ${}^6\text{Li}$ projectiles, shown in Fig. 5, we note that the contribution from the SCF cross section is appreciable, reaching almost 40% of the contribution from DCF. This is in line with the observation that breakup should be more important in the case of this more weakly bound nucleus.

Now we compare the calculated ICF cross sections with the corresponding experimental data. We remark that the experimental data are, in fact, the cross sections for production of nucleides with atomic numbers one (ICF of ${}^2,{}^3\text{H}$) or two (ICF of ${}^4\text{He}$) units higher than that of Bi, namely, At and Po isotopes. Therefore, the data include also direct transfer of the ${}^2,{}^3\text{H}$ and ${}^4\text{He}$ clusters. The results for the ${}^7\text{Li}$ and ${}^6\text{Li}$ projectiles are shown, respectively, in Figs. 6 and 7. In both cases, and especially for the ${}^7\text{Li}$ projectiles, the agreement between experiment and theory is poor. The direct transfer of clusters may be responsible, for the discrepancies, at least in part. However, to clarify this point it would be necessary to perform a very complicated and time-consuming semiclassical calculation, including also several transfer channels. We notice that the transfer process appears to be especially dominant for ${}^7\text{Li}$ projectiles. This is because of the larger number of transfer channels open in this case.

FIG. 6. (Color online) Comparison of the contribution from transfer and ICF channels in reactions induced by ${}^7\text{Li}$ projectiles to the calculated cross section from ICF processes.FIG. 8. (Color online) Contributions from the ${}^3\text{H}$ (short-dashed line) and ${}^4\text{He}$ (long-dashed line) fragments of ${}^7\text{Li}$ to the calculated ICF cross section (solid line) in the ${}^7\text{Li}-{}^{209}\text{Bi}$ collision.

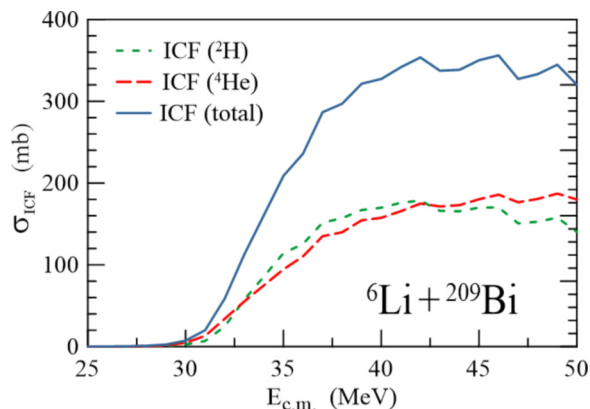


FIG. 9. (Color online) Contributions from the ${}^2\text{H}$ (short-dashed line) and ${}^4\text{He}$ (long-dashed line) fragments of ${}^6\text{Li}$ to the calculated ICF cross section (solid line) in the ${}^6\text{Li}-{}^{209}\text{Bi}$ collision.

To finish this section, we discuss the contribution from each breakup fragment to the ICF cross section. We consider the ${}^7\text{Li}-{}^{209}\text{Bi}$ and ${}^6\text{Li}-{}^{209}\text{Bi}$ collisions, for which the fragments are, respectively, $[{}^3\text{H}, {}^4\text{He}]$ and $[{}^2\text{H}, {}^4\text{He}]$. The experiment of Ref. [3] measured separate cross sections for most Po and At isotopes, which are, respectively, the signatures for the absorption of H and He. However, it cannot distinguish between ${}^{210}\text{Po}$ and ${}^{210}\text{At}$. The reason is that ${}^{210}\text{At}$ decays to ${}^{210}\text{Po}$ with $T_{1/2} = 8.3$ h and the cross section of ${}^{210}\text{Po}$, which decays with $T_{1/2} = 138$ d, was determined from off-line spectra accumulated during a few days. Thus, the measurements give, in fact, the summed cross sections for these two nuclei. Because this result corresponds to most of the experimental ICF cross section, there are no reliable data on the contribution from each fragment. For this reason, we base our discussion exclusively on the calculated cross sections.

Figures 8 and 9 show, respectively, the calculated ICF cross sections for the two ${}^7\text{Li}$ and ${}^6\text{Li}$ projectiles (solid lines). The contributions from the breakup fragments are represented by short- and long-dashed lines, as indicated in the legends and captions of the figures. In the case of ${}^7\text{Li}$, the contributions from the two fragments are similar at low energies but at higher energies the contribution from ${}^4\text{He}$ is twice as large. In the case of ${}^6\text{Li}$, the contributions from ${}^2\text{H}$ and from ${}^4\text{He}$ are similar in the whole energy range.

IV. CONCLUSIONS

We have developed a semiclassical calculation procedure to study the influence of the breakup process in the fusion reaction of a weakly bound projectile with a heavy target.

We have applied it to ${}^6,{}^7\text{Li} + {}^{209}\text{Bi}$ collisions at near-barrier energies and compared its predictions for the CF and TF cross section with the data of Dasgupta *et al.* [2]. Our model was shown to reproduce the CF data. Further, our results indicate a sizable contribution of the SCF process to the total CF cross section in the case of ${}^6\text{Li}$ projectiles, indicating that an improper consideration of this process may lead to inaccurate predictions of both the complete and incomplete fusion cross sections.

Furthermore, we have encountered large differences between the predictions of the TF cross sections of our calculations and those reported in the data. We argue that this may be attributable to the contributions from direct transfer processes to the yields of final nuclei that cannot be distinguished from those of true ICF events.

Our calculations are subject to refinements, as they are based on a series of simplifying assumptions. The quality of the description of available data on CF indicates that the semiclassical method has the potential to give a complete and accurate picture of the processes occurring in collisions induced by weakly bound nuclei, and other similar systems. In particular, they could be applied to study collisions between molecules, atomic clusters, and other objects for which the small de Broglie wavelength of the relative motion justifies the use of a classical trajectory, while the internal states of the colliding partners require a quantal description. We stress that quantum-mechanical CDCC calculations for systems like ${}^6\text{Li} + {}^{209}\text{Bi}$ cannot evaluate separate cross sections for CF and ICF [11]. Thus, this seems to be an important strength of the semiclassical approach. The purely classical treatment [5,6] is able to correctly distinguish between all of these processes, but lacks, however, the inclusion of quantum effects, such as tunneling, which are known to be an important ingredient in fusion processes, and, most importantly, the quantum-mechanical description of the excitation of the weakly bound projectile during the collision process.

ACKNOWLEDGMENTS

We thank Dr. Paulo Gomes from the Universidade Federal Fluminense for useful discussions and suggestions and Dr. Pablo Ezzatti from the Instituto de Computación, Facultad de Ingeniería, for important computational support. We acknowledge partial financial support from CAPES, Conselho Nacional de Desenvolvimento Científico e Tecnológico (CNPq), FAPERJ and FAPERJ/CNPq (PRONEX), under Contract No. 41.96.0886.00, Fundação de Amparo à pesquisa do Estado de Rio de Janeiro, and PEDECIBA and ANII (Uruguay).

- [1] L. F. Canto, P. R. S. Gomes, R. Donangelo, and M. S. Hussein, *Phys. Rep.* **424**, 1 (2006).
 [2] M. Dasgupta, D. J. Hinde, K. Hagino, S. B. Moraes, P. R. S. Gomes, R. M. Anjos, R. D. Butt, A. C. Berriman, N. Carlin, C. R. Morton *et al.*, *Phys. Rev. C* **66**, 041602(R) (2002).

- [3] M. Dasgupta, P. R. S. Gomes, D. J. Hinde, S. B. Moraes, R. M. Anjos, A. C. Berriman, R. D. Butt, N. Carlin, J. Lubian, C. R. Morton *et al.*, *Phys. Rev. C* **70**, 024606 (2004).
 [4] M. Dasgupta, D. J. Hinde, R. D. Butt, R. M. Anjos, A. C. Berriman, N. Carlin, P. R. S. Gomes, C. R. Morton, J. O. Newton, A. Szanto de Toledo *et al.*, *Phys. Rev. Lett.* **82**, 1395 (1999).

- [5] K. Hagino, M. Dasgupta, and D. J. Hinde, *Nucl. Phys. A* **738**, 475 (2004).
- [6] A. Diaz-Torres, *Comput. Phys. Commun.* **182**, 1100 (2011).
- [7] K. Hagino, A. Vitturi, C. H. Dasso, and S. M. Lenzi, *Phys. Rev. C* **61**, 037602 (2000).
- [8] A. Diaz-Torres and I. J. Thompson, *Phys. Rev. C* **65**, 024606 (2002).
- [9] A. Diaz-Torres, I. J. Thompson, and C. Beck, *Phys. Rev. C* **68**, 044607 (2003).
- [10] N. Keeley, K. W. Kemper, and K. Rusek, *Phys. Rev. C* **65**, 014601 (2001).
- [11] K. Keeley and N. Rusek, *Phys. Lett. B* **375**, 9 (1996).
- [12] H. D. Marta, L. F. Canto, and R. Donangelo, *Phys. Rev. C* **78**, 034612 (2008).
- [13] H. D. Marta, L. F. Canto, R. Donangelo, and P. Lotti, *Phys. Rev. C* **66**, 024605 (2002).
- [14] F. M. Nunes and I. J. Thompson, *Phys. Rev. C* **57**, R2818 (1998).
- [15] F. M. Nunes and I. J. Thompson, *Phys. Rev. C* **59**, 2652 (1999).
- [16] R. A. Broglia and A. Winther, *Heavy Ion Reactions* (Westview Press, Boulder, CO, 2004).
- [17] P. R. Christensen and A. Winther, *Phys. Lett. B* **65**, 19 (1976).
- [18] D. H. Luong, M. Dasgupta, D. J. Hinde, R. du Rietz, R. Rafiei, C. J. Lin, M. Evers, and A. Diaz-Torres, *Phys. Rev. C* **88**, 034609 (2013).
- [19] A. Shrivastava, A. Navin, N. Keeley, K. Mahata, K. Ramachandran, V. Nanal, V. V. Parkar, A. Chatterjee, and S. Kailas, *Phys. Lett. B* **633**, 463 (2006).
- [20] D. H. Luong, M. Dasgupta, D. J. Hinde, R. du Rietz, R. Rafieri, C. J. Lin, M. Evers, and A. Diaz-Torres, *Phys. Lett. B* **695**, 105 (2011).